

Colloidal and microfluidic nematic microstructures

Simon Čopar,¹ Miha Ravnik,^{1,2} and Slobodan Žumer^{*2,1}

¹*Faculty of Mathematics and Physics, University of Ljubljana, Slovenia*

²*J. Stefan Institute, Ljubljana, Slovenia*

In this review paper, we give a selected review on colloidal and microfluidic nematic microstructures, as enabled by the inherent anisotropy and microscopic orientational ordering in complex liquid crystalline materials. We give a brief overview of the mesoscopic theory – for equilibrium and dynamics – of nematic fluids, that provides the framework for understanding, characterisation and even prediction of such microstructures, with particular comment also on the role of topology and topological defects. Three main types of nematic microstructures are highlighted: stable or metastable structures in nematic colloids, stationary nematic microfluidic structures, and ferromagnetic liquid crystal structures. Finally, this paper is in honour of Noel A. Clark as one of the world pioneers that helped to shape this field of complex and functional soft matter.

I. INTRODUCTION

Liquid crystals discovered in late nineteenth century attracted attention for a long period as materials with fascinating optical textures. Much later in the late fifties to early seventies of 20th century liquid crystals started to attract physicists that developed basic understanding of the related physics [1–5]. In parallel, the applied oriented researchers set the ground for twisted nematic liquid crystal displays [6, 7]. After a slow start, the nematic based displays became the dominate display technology in last 20 years [8]. In the seventies, also Noel Clark as a postdoc was attracted to the fast growing field devoted to the physics of liquid crystals. He started with light scattering and dynamics of nematics [9] and thin smectic layers [10]. With his pioneering research of sub microsecond switching of smectic liquid crystals [11] that was also the base for the development of the ferroelectric liquid crystal display [12] he became well known. Following his diverse interests, Noel Clark spread the activities of his lab to a broad range of soft matter systems far beyond smectic liquid crystals and his lab became one of the leading places in the field of liquid crystal related research. His research includes lyotropic lamellar phases [13], nematics in random porous media [14], bent core liquid crystals [15], nematic colloidal crystals as possible photonic crystals [16], DNA based biological phases [17], helical nanofilament phases [18], heliconical nematics [19], and recently colloidal nematic ferromagnets [20].

In our review we focus on topological aspects of nematic defect structures formed in colloidal and confined fluidic liquid crystal systems where some segments of Noel Clark’s research closely relate to the topics of our review. Topological aspects of nematic liquid crystals were first set in a broader context nearly 50 years ago [21–24]. The discovery of polymer dispersed liquid crystals [25] stimulated research of liquid crystals in diverse geometries ranging from spherical droplets to regular cylindrical pores and random porous networks [14, 26, 27]. Similarly, the interest in systems with inverse geometry — liquid crystal colloids — with particle sizes ranging from few nanometers to several micrometers started to grow. The study of a single spherical particle inducing homeotropic anchoring in a nematic host identified the Saturn ring structure with $-1/2$ disclination loop and in the case of planar anchoring the structure with boojum defects on the two poles [28]. More detailed studies showed that in the homeotropic case also asymmetric structure with a hyperbolic hedgehog exists, what widened the possibilities for different inter particle interactions in such colloidal dispersions [29–32]. This stimulated the formation of various 2D nematic colloidal lattices [33, 34], 3D lattices [35] and also structures in complex confinement [36]. The discovery that disclination lines can entangle more than one supra micrometer size colloidal particle [37] and the understanding of its topological description [38] led to the realization and understanding of the knotting and linking of large 2D assemblies of colloidal particles in thin nematic layers [39]. Similar approach explained also disclination structures appearing in 3D interconnected system of pores infiltrated by a nematic [40, 41]. A system of densely packed colloidal spheres infiltrated by a nematic that had been introduced earlier by Noel A. Clark [16] was explained by the same topological approach [42]. Further broadening of the liquid crystal colloidal research came with shaped particles and particles characterised by specific physical properties. The introduction of shaped platelets [43] allowed formation of quasi-crystalline tilings [44]. The use of long cylindrical objects led to complex surface defect structures [45] and dispersions of cylindrical particles together with surface charges to triclinic colloidal lattices [46]. Forming of colloidal particles in shapes of various handlebodies was used as an example of a complex nematic defect topology [47]. Use of 3D printing allowed for formation of knotted and linked colloidal particles on micron scale that in the nematic host formed mutually tangled, linked particle-field knots, and could also organize in a colloidal lattice [48, 49]. Another interesting example were golden particles in the form of mesoflowers that in a nematic host induce elastic deformations of higher elastic multipoles [50]. Using magnetism concepts, magnetic particles in the shape of platelets with nanoscale thickness were demonstrated that formed ferromagnetic nematic colloidal dispersions [51]. Noel Clark with coworkers has recently shown that even

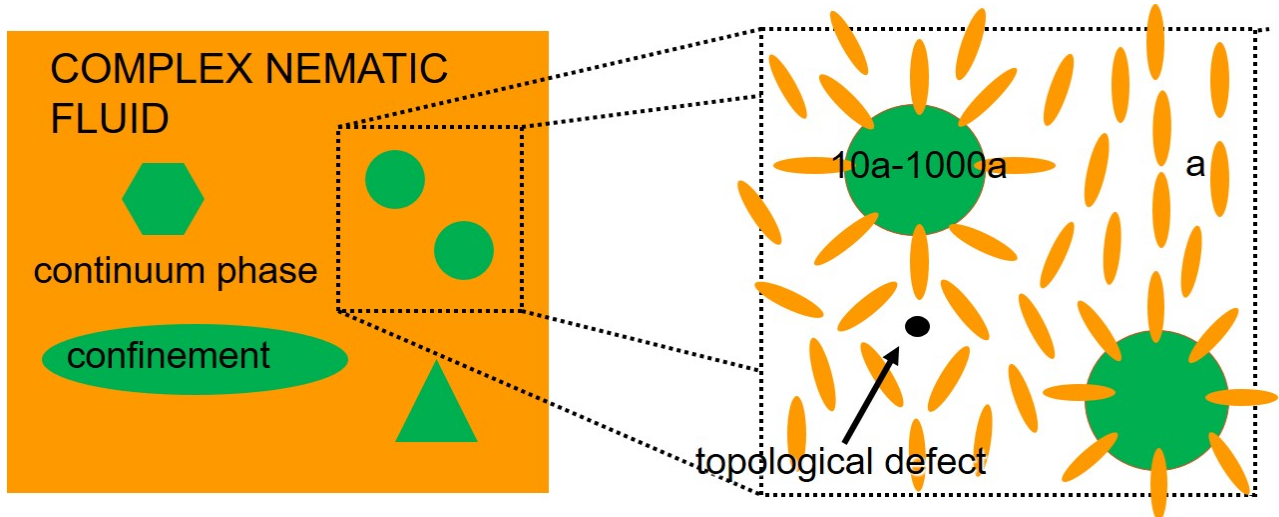


FIG. 1: Schematic representation of complex nematic structures. Orange shows continuum liquid crystal phase consisting from nematic agents denoted with a . Green indicates general confinement which can be imposed either by different surfaces, such as particles and channel or cell walls. A scheme of $-1/2$ topological defect is shown in black.

a dispersion of magnetic platelets in an isotropic fluid at certain concentrations leads to a colloidal nematic liquid crystal with ferromagnetic properties [20].

The studies of dynamics of liquid crystals started with the development of physical understanding of these phases. It soon became clear that reorientation of the director is accompanied by flow and reversed coupling known as backflow mechanism [52, 53]. For fluctuations reorientation angles are small and flow effects can be neglected [5, 9], while they are crucial for switching of a nematic in displays [54, 55]. Many studies are also devoted to driven liquid crystalline systems like convection instabilities [56, 57] and recently to active systems that for example exhibit active nematic turbulence [58]. In this review, we focus only to studies where microfluidics in certain confining geometries can generate stationary topological defect structures [59].

Our review has the following structure: introduction, mesoscopic approach to nematic complex fluids, Landau-de Gennes free energy approach, nematodynamics, topological defects, nematic colloids, nematic colloidal assemblies, stationary nematic microfluidic structures, ferromagnetic liquid crystal structures, and conclusions.

II. MESOSCOPIC APPROACH TO NEMATIC COMPLEX FLUIDS

Nematic liquid crystal fluids exhibit orientational order with building blocks aligning along some common direction, usually referred to as director \mathbf{n} with directions \mathbf{n} and $-\mathbf{n}$ being equivalent. The director is a vectorial-like order parameter, which corresponds to the time or ensemble average of molecular orientations \mathbf{a} (see Fig. 1). Nematic degree of order (scalar order parameter) S is introduced as another order parameter which measures the local fluctuations in the orientation of the nematic building blocks. The full orientational order of liquid crystals is described by the tensor order parameter Q_{ij} , that contains degree of order S , director \mathbf{n} and also possible biaxiality P as $Q_{ij} = \frac{S}{2} (3n_i n_j - \delta_{ij}) + \frac{P}{2} (e_i^{(1)} e_j^{(1)} - e_i^{(2)} e_j^{(2)})$, where $\mathbf{e}^{(1)}$ is the secondary director (perpendicular to \mathbf{n}) that characterises the biaxial ordering, and $\mathbf{e}^{(2)} = \mathbf{n} \times \mathbf{e}^{(1)}$ [5].

A. Landau-de Gennes free energy approach

A strong theoretical and modelling mesoscopic approach to equilibrium properties of nematic fluids is to use the minimisation of the Landau-de Gennes free energy $F = \int f dV$, with f being the free energy volume density written as a sum of effective ordering and elastic terms $f = f_S + f_E$ [60]. The first contribution f_S accounts for the variability of the nematic degree of order whereas the second contribution f_E accounts for the spatial elastic deformations of the

nematic ordering. They are written as:

$$f_S = \frac{1}{2}A Q_{ij}Q_{ji} + \frac{1}{3}B Q_{ij}Q_{jk}Q_{ki} + \frac{1}{4}C(Q_{ij}Q_{ji})^2, \quad (1)$$

$$f_E = \frac{1}{2}L_1 \frac{\partial Q_{ij}}{\partial x_k} \frac{\partial Q_{ij}}{\partial x_k} + \frac{1}{2}L_2 \frac{\partial Q_{ij}}{\partial x_j} \frac{\partial Q_{ik}}{\partial x_k} + \frac{1}{2}L_3 Q_{ij} \frac{\partial Q_{kl}}{\partial x_i} \frac{\partial Q_{kl}}{\partial x_j}, \quad (2)$$

where A , B , and C are nematic order material parameters, L_1 , L_2 and L_3 are tensorial elastic constants, x_i are Cartesian coordinates and summation over repeated indices is assumed. Parameter A usually contains temperature dependence as $A = a(T - T^*)$ (but could also be density dependent) and governs the nematic to isotropic transition. Three elastic constants are needed to quantify the three standard nematic elastic modes (splay, twist and bend). If one assumes uniaxial approximation of the order parameter tensor \mathbf{Q} ($S = \text{const.}$ and $P = 0$), the free energy density f_E can be rewritten into the Frank-Oseen free energy form by mapping the tensorial constants L_i to Frank elastic constants K_i (which are usually measured in experiments) [61], as

$$K_1 = \frac{9S^2}{4}(2L_1 + L_2 - L_3S), \quad (3)$$

$$K_2 = \frac{9S^2}{4}(2L_1 - L_3S), \quad (4)$$

$$K_3 = \frac{9S^2}{4}(2L_1 + L_2 + 2L_3S). \quad (5)$$

The minimisation of the total free energy F gives the -stable or metastable- equilibrium of the system and is usually performed using different numerical methods, such as finite difference relaxation algorithms or finite elements [62, 63]. The particular strength of the free energy minimisation approach is that other free energy contributions corresponding to other material mechanisms or couplings can be directly added, such as surface anchoring, coupling to electric or magnetic fields, flexoelectricity or ionic effects [57, 60, 64].

B. Nematodynamics

Hydrodynamics of nematic liquid crystals is centrally determined by the coupling between the nematic orientational ordering given by the nematic order tensor Q_{ij} or director n_i , and the material flow, usually given by the material velocity flow field v_i . The flow field of nematic is given by the generalised Navier-Stokes equation

$$\rho \left[\frac{\partial v_i}{\partial t} + (v_j \partial_j) v_i \right] = \partial_j \sigma_{ij}, \quad (6)$$

where ρ is the density, v_i the velocity, and σ_{ij} the stress tensor which includes beside the standard pressure also the dependence on the anisotropic nematic order in the system. The stress tensor can be written as a sum of the Ericksen stress tensor $\sigma_{ij}^{\text{Er}} = -\frac{\delta \mathcal{F}}{\delta \partial_j Q_{kl}} \partial_i Q_{kl} - (p_0 - f) \delta_{ij}$ which includes the elasticity effects (p_0 is the external pressure), and viscous stress tensor $\sigma_{ij}^{\text{viscous}}$ which depends on the actual nematic order as well as its time derivative. Such dependence of the stress tensor directly implies that in principle any time-variation of the nematic order induces materials flows, both in the process of the relaxation towards equilibrium or if driven by the time-varying external fields. As part of the mesoscopic approach to nematodynamics, the generalised Navier-Stokes equation and incompressibility ($\partial_j v_j = 0$) are complemented by the equation for the evolution of the nematic order parameter, written either in the director or in the Q tensor form. There are two established formulations of the nematic order parameter tensor based nematodynamic models – the Beris-Edwards model [65] and Qian-Sheng model [66].

Beris and Edwards formulate their equations for nematic hydrodynamics through tensorial description of nematic order, where they utilize a generalization of the Poisson bracket description of thermodynamics [65]. In a typical formulation, their equations are written as [67, 68]:

$$\dot{Q}_{ij} = S_{ij} + \Gamma H_{ij}, \quad (7)$$

$$\begin{aligned} S_{ij} = & (\zeta A_{ik} - \Omega_{ik}) \left(Q_{kj} + \frac{\delta_{kj}}{3} \right) + \left(Q_{ik} + \frac{\delta_{ik}}{3} \right) (\zeta A_{kj} + \Omega_{kj}) \\ & - 2\zeta \left(Q_{ij} + \frac{\delta_{ij}}{3} \right) Q_{kl} \frac{\partial v_k}{\partial x_l}, \end{aligned} \quad (8)$$

$$\begin{aligned}\sigma_{ij}^{\text{viscous}} = & -\zeta H_{ik} \left(Q_{kj} + \frac{\delta_{kj}}{3} \right) - \zeta \left(Q_{ik} + \frac{\delta_{ik}}{3} \right) H_{kj} + 2\zeta \left(Q_{ij} + \frac{\delta_{ij}}{3} \right) Q_{kl} H_{kl} \\ & + Q_{ik} H_{kj} - H_{ik} Q_{kj} + 2\eta A_{ij},\end{aligned}\quad (9)$$

where $\Omega_{ij} = (\partial_i v_j - \partial_j v_i)/2$ and H_{ij} is the molecular field defined as:

$$H_{ij} = -\frac{1}{2} \left(\frac{\delta \mathcal{F}}{\delta Q_{ij}} + \frac{\delta \mathcal{F}}{\delta Q_{ji}} \right) + \frac{1}{3} \frac{\delta \mathcal{F}}{\delta Q_{kk}} \delta_{ij}. \quad (10)$$

Beris-Edwards model as formulated above has three independent viscosity parameters Γ , ζ , and η , which relate to the six Leslie viscosities (of which 5 are independent). Rotational diffusion constant Γ sets up the typical timescale of the dynamical processes in the nematic at a given length scale, ζ is the alignment parameter and prescribes the Leslie angle in the shear flow or tumbling nature of the nematic, and η determines the isotropic viscosity of the system.

Nematodynamic model formulated by Qian and Sheng [66] follows the formalism of thermodynamic fluxes and forces, within the description of the tensorial nematic order. Viscous stress tensor is written as:

$$\begin{aligned}\sigma_{ij}^{\text{viscous}} = & \beta_1 Q_{ij} Q_{kl} A_{kl} + \beta_4 A_{ij} + \beta_5 A_{ik} Q_{kj} + \beta_6 Q_{ik} A_{kj} \\ & + \frac{1}{2} \mu_2 N_{ij} - \mu_1 N_{ik} Q_{kj} + \mu_2 Q_{ik} N_{kj},\end{aligned}\quad (11)$$

where $N_{ij} = \dot{Q}_{ij} + \Omega_{ik} Q_{kj} - Q_{ik} \Omega_{kj}$ is the corotational derivative of the Q-tensor. Time evolution of the Q-tensor is given by

$$\dot{Q}_{ij} = \frac{H_{ij}}{\mu_1} - \frac{\mu_2 A_{ij}}{2\mu_1} + Q_{ik} \Omega_{kj} - \Omega_{ik} Q_{kj}. \quad (12)$$

The model is formulated with six viscosity coefficients $\beta_1, \beta_4, \beta_5, \beta_6, \mu_1$, and μ_2 , linked by relation $\beta_6 - \beta_5 = \mu_2$. The number of coefficients is exactly the same as in the director based Ericksen-Leslie nematodynamic model, and at a constant degree of order, coefficients can be exactly mapped between the two models.

A strong way for characterisation of the nematic flow is to construct a relevant dimensionless numbers, especially, to characterise the coupling between the flow and orientational order. In experiments and simulation involving nematic flow, Reynolds number is typically much smaller than 1. Therefore, a better insight into nematic nature of flow is given by the Ericksen number which compares the nematic elastic forces to the viscous forces, and is given as $\text{Er} = \frac{\gamma_1 v/l}{K/l^2} = \frac{\gamma_1 v l}{K}$, where v is a typical flow velocity in the system, l is the typical length scale, and K is the single Frank elastic constant. At small Ericksen numbers, the director dynamics is governed by the elastic terms, whereas at large Ericksen numbers the dynamics is dictated by the velocity profile. Typical values for Ericksen number are $\text{Er} \sim 1$ when considering annihilation of defect pairs [69, 70] or moderately slow flow in microchannels [71] and $\text{Er} \sim 20$ for strong flow in microchannels [71]. These nematodynamic models — either Beris-Edwards or Qian-Sheng formulation — are usually solved numerically by different numerical methods, such as Lattice Boltzmann methods [72, 73], finite elements [74] or multi-particle collision dynamics [75, 76].

III. TOPOLOGICAL DEFECTS AND NEMATIC COLLOIDS

Elastic penalty for variations in the orientational order of the nematic liquid crystals imposes the director to be a continuous, preferably a slowly varying function. However, this is not always achievable as some boundary conditions or strong coupling to external field or flow are incompatible with a continuously varying director across the entire domain. Instead, defects must be present in the bulk, set by the topological constraints. Nematics can feature two types of these topological defects — point defects and line defects. Being a line field — a unit vector field with head-tail equivalence — each nematic sample is a function mapping from the real space, occupied by the liquid crystal, to the real projective plane. Defects can be labeled by the homotopy groups, which also provide the conservation laws for the associated topological charges. The application of this formalism to understanding of experimental behaviour has been developed and studied by researchers, such as Mermin, Kleman and others [23, 26, 77, 78].

Disclination lines are classified by encircling them with a virtual loop, and measuring how many turns the director makes while moving along the loop, which gives the winding number of the disclination. The fundamental group of the real projective plane, $\pi_1 = \mathbb{Z}_2$, only allows for two options — the case without disclinations, and the half-integer winding corresponding to defects with a singular core.

Looking in three spatial dimensions, simple point defects, compound defects made of one or more defect loops and point defects, or inclusions, such as colloidal particles and droplets, can be assigned an integer called topological

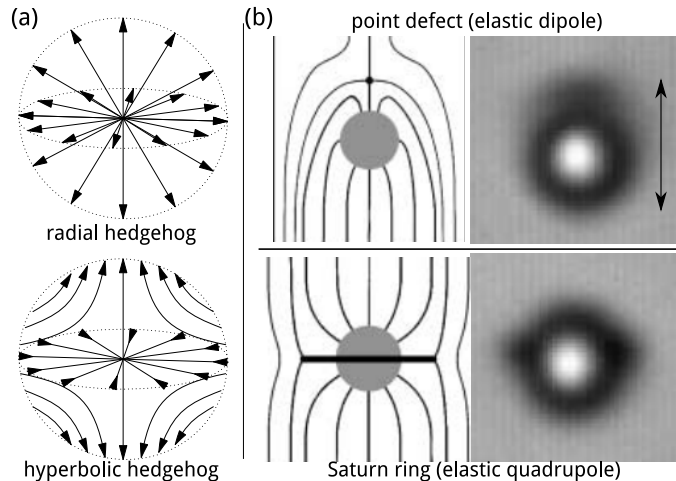


FIG. 2: Topological charge. (a) The simplest nematic point defects – the radial and hyperbolic hedgehog. (b) A colloidal particle with an accompanying defect, forming an elastic dipole and an elastic quadrupole (images adapted from [33]).

charge. This charge can be determined by wrapping the object with a sphere, and counting how many times the director on the sphere points into each spatial direction. The second homotopy group of the real projective plane, $\pi_2 = \mathbb{Z}$, dictates that these charges are additive.

The simplest object with a nonzero topological charge is a colloidal particle with homeotropic (perpendicular) surface anchoring, for example, a silica microparticle with a DMOAP surface treatment. In a nematic, the field immediately around this particle points in every direction in space, hence it has a topological charge of $+1$ (where the sign is by agreement). In a nematic with a uniform far-field, for example in a planar cell, such a particle will be accompanied by topological defects, either a hyperbolic hedgehog – a point defect with a topological charge of -1 , or by a closed disclination loop also called Saturn ring [28, 29, 31]. Based on the symmetry of the surrounding director field, these are also called the elastic dipole and elastic quadrupole [30, 79], respectively (see Fig. 2).

The spherical shape is topologically nontrivial with its nonzero Euler characteristic, and thus induces defects. In an inverted case of homeotropic nematic droplets (usually in an aqueous host), the topological charge inside the droplet must total $+1$. Nematic drops have been studied for a long time [80], but are so rich in behaviour, especially when chirality is involved [81]. For example, in cholesteric droplets, new higher-order point defects with topological charge different from ± 1 , previously thought impossible, have been experimentally observed [82, 83], opening new mathematical questions in the process [84].

The homotopy formalism and topological charges are well applicable for most of rather simple cases (geometries), but for example, interactions of line and point defects in the same system leads to additional complications, as the first and second homotopy group are not independent. This became increasingly important in nematic emulsions and colloids [29] and more recently also in active nematics [58]. Inclusions in the nematic host introduce a topologically nontrivial domain that induces a mixture of point defects, closed line defect loops, which may be linked or knotted. Closed disclination loops carry also a point topological charge, and conversely, disclination loops make the topological charges on individual point defects in the system no longer additive [85, 86]. Description of such systems warrants a more complete description that takes into account not only topological charges of individual defects, but considers the global topology of the entire nematic sample [87, 88].

Disclination lines can formally have any varying cross sectional profile, but elastic free energy cost places energetic restrictions on them, and around particles. Therefore, in many cases, they have a constant profile of winding number, such as the $-1/2$ winding number (Fig. 3a). Such disclinations can be thought of as framed curves, a kind of three-fold ribbon owing to the three-fold symmetry of their cross section. When they are closed into loops, they can be assigned an additional topological invariant – the self-linking number, which counts the total number of turns along the loop [38] (Fig. 3b). The three-fold symmetry allows self-linking in multiples of $1/3$. Odd multiples of $1/3$ must be linked by an odd number of other disclination loops, and even multiples of $1/3$ can exist unlinked and alternate between even and odd topological point charge. The complete conservation law, taking into account any number n of possibly linked loops with linking numbers Lk_{ij} , can be written as

$$\frac{3}{2} \left(\sum_i^n \text{Sl}(A_i) + \sum_{i \neq j}^n \text{Lk}(A_i, A_j) \right) + n = q \mod 2. \quad (13)$$

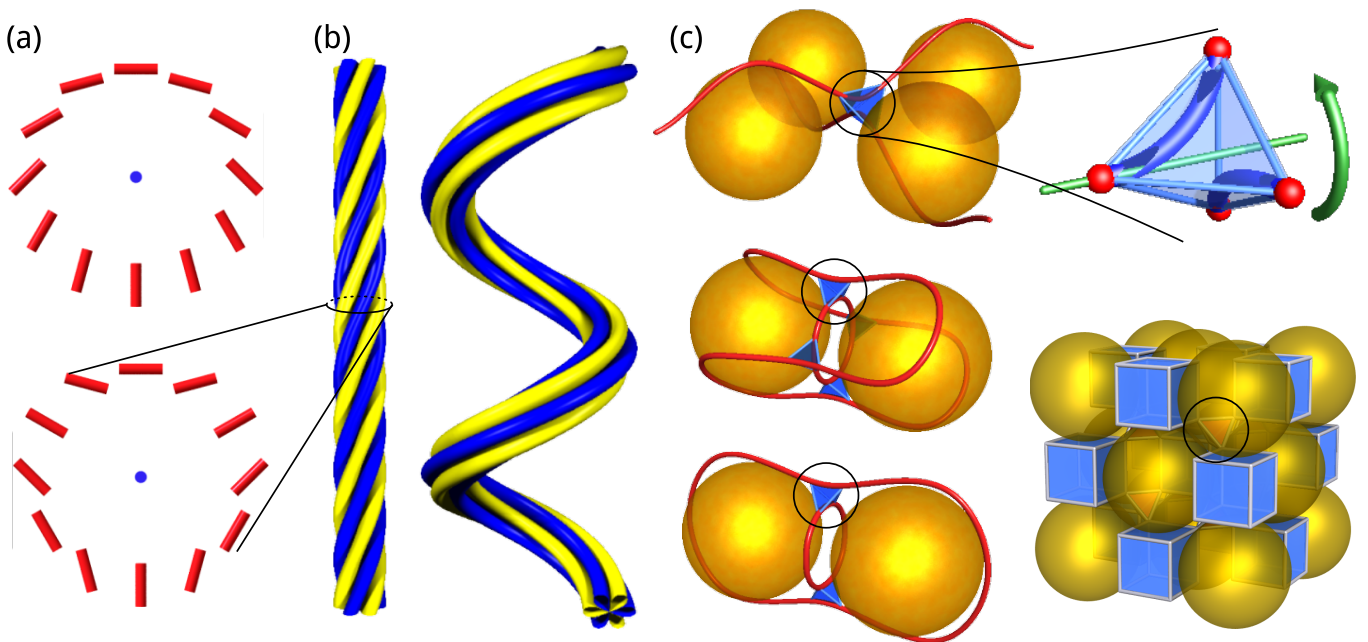


FIG. 3: Topology of disclination lines. (a) Disclinations with planar cross sections with winding numbers $+1/2$ and $-1/2$. (b) Disclination lines with $-1/2$ can twist or writhe, accumulating self-linking SI when closed into a loop. (c) Disclinations can be reconfigured in three different ways at possible selected rewiring sites, which for example can emerge in different nematic colloidal assemblies.

Here, q is the topological charge of the entire system of disclination loops. The modulo 2 is there because the presence of disclination lines prevents consistent assignment of arrows to the nematic director field – there is no well defined global topological charge conversation apart from the parity.

The theory can be generalized to account for changes of disclination profile along the loop [89], which is relevant, for example, for hybrid disclinations formed when connecting Saturn-ring defects to defects around cylindrical inclusions [45], and in active nematics, where disclination loops dynamically transform and stretch, with self-propulsion velocity dependent on the local disclination profile [90]. More generally, in chiral liquid crystals (cholesterics), classification of disclination lines is more complex, as their type depends on whether the director, the helical axis, or both, have a nonzero winding number [91].

The three-fold ribbon description of disclination lines is well suited for describing rewiring of disclinations [38, 92]. Entangled and knotted disclination lines that span multiple inclusions [37, 39], can be difficult to understand, but noticing that each pair of closely passing disclination line segments can be identified as a potential rewiring site, implies that many different disclination line configurations, together with the surrounding director field, are similar everywhere except in the rewiring (tetrahedral) region. Rotating the tetrahedron and the field inside it by 120° increments, rewires the disclination network and changes the cumulative self-linking number by $\pm 2/3$. Even with just two spheres, we can observe entanglement and rewiring, which can be readily performed by targeted application of optical tweezers [37] (Fig. 3c). Tetrahedral rotations are natural moves to describe the changes in topology of the loop itself, as they correspond to tangles in planar knot diagrams, used in calculation of knot invariants [39, 93]. The presence of surrounding nematic field imparts additional structure on the conventional knot theory, which was explored later by Machon et al. [94].

IV. NEMATIC COLLOIDAL ASSEMBLIES

Topological defects can appear transiently after a quench or in flow, but as approaching equilibrium or steady state, they tend to annihilate to reduce the elastic deformations and their free energy, unless stabilized by boundary conditions and geometry of the confining space. This is readily seen in porous structures infused by a nematic. Branched networks of channels treated to enforce a particular boundary condition, provide a multitude of places where defects are topologically required, leading to multistability and thus switchability of the resulting composite material [14, 40–42, 95, 96]. Surface topography, such as holes or pillars, can be used either to induce uniform order

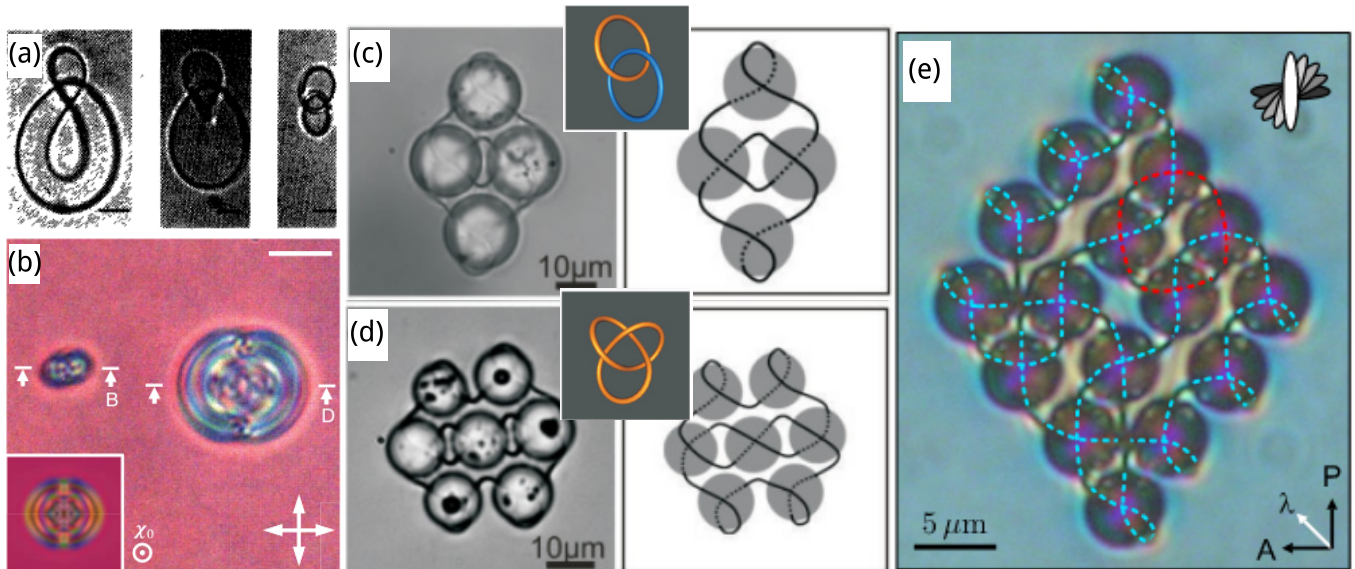


FIG. 4: Knotted and linked disclinations in cholesterics and nematics. (a) Transient linked cholesteric disclinations, observed by Yves Bouligand [107]. (b) A stable knotted cholesteric disclination, by Tai et al. [108]. (c,d) Linked and knotted disclinations stabilized by silica microspheres in a π -twisted cell [109]. (e) A complex link stabilized in a $\pi/2$ -cell on a nematic 2D colloidal crystal grid [93].

at the surface [97], or to stabilize defects and specific director patterns, which can act as optical devices or sensors [98–101]. However, these cases all rely on static geometry to support a director field. The possibilities greatly expand, when the confinement is enforced by freely movable particles, which themselves are guided and assembled by the director field around them. – the nematic colloids [33, 39, 47, 48, 102, 103]. Due to the strong relevance of topology, these composites can also be placed into broader category of topological soft matter.

Monodisperse silica spheres treated with DMOAP to achieve homeotropic surface anchoring have been shown to produce different defect conformations, depending on the type of the nematic cell, confinement ratio between the sphere diameter and cell thickness, and the size of the particles [103]. The topological defects act as force mediators, and can assemble many different arrangements based on the type of defects and the geometry of the confinement. Particles with point defects and Saturn rings assemble loosely at a distance into dipolar, quadrupolar [33] or mixed crystals [104] (Fig. 5a-c). Particles entangled with a single-stroke disclination line around them, are more tightly bound, because the disclination acts as an elastic string with an approximately constant tension. In a twisted nematic cell, the tetrahedral rewiring sites are position in a way that allows rewiring in two dimension, hence allowing for made-to-order of diverse knots or links [39] (Fig. 5d).

Chirality supports creation of complex disclination geometries, as preferred disclination direction varies along the helical axis (Fig. 4). In a π -twisted cell, complex knots and links can be achieved around a smaller number of particles [109]. In chiral samples, knotted disclination lines can be observed even without the stabilizing effect of particles. Transient linked disclinations have been observed already by Y. Bouligand [107] during coarsening. Later, stable knotted structures have been created in cholesteric cells [108] and predicted in cholesteric droplets [81].

Nematic colloidal inclusions with non-spherical particles are explored. Notable examples of non-spherical colloids are dispersions of rods [110], polygonal particles [111], handlebodies [47], knots and links [48, 112], irregular shapes [113–117], fractals [118], and particles that can change their shapes [49] (Fig. 6). An interesting application for suspensions of oddly shaped particles are optical metamaterials, which need regular alignment and spacing. A nematic can provide this self-assembly with its elasticity and topological defects [120, 121], or the particles themselves can form a nematic order owing to their shape [122].

To generalise, the field of nematic colloids can involve a multitude of interconnected phenomena, which can be tuned and designed [123] to a certain need to produce a material with desired function.

V. STATIONARY NEMATIC MICROFLUIDIC STRUCTURES

Nematic microfluidic structures are crucially determined by the backflow coupling between the material flow and the nematic orientational order. As the results of this coupling, different transient, stationary or static liquid crystal

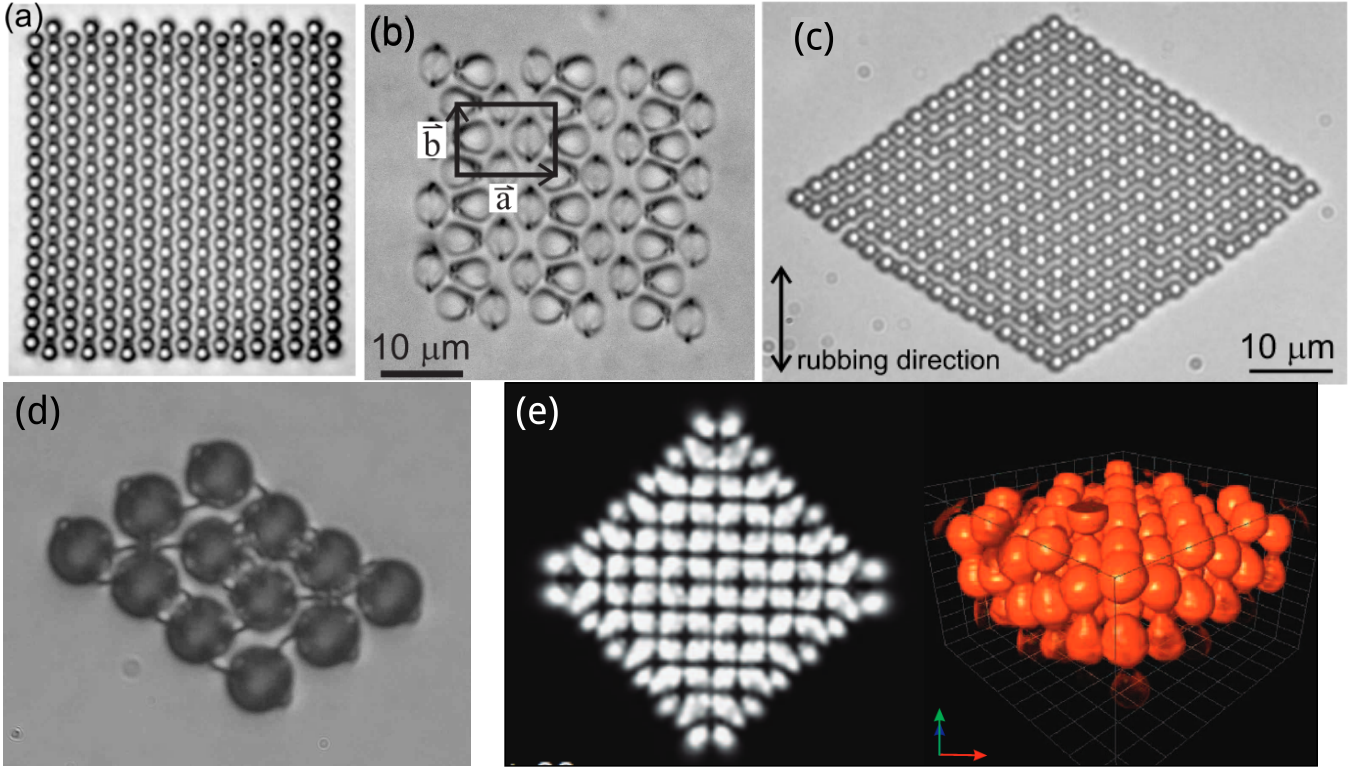


FIG. 5: Colloidal assemblies of spherical microparticles in a nematic under different confinement conditions. Two-dimensional crystals can be formed from (a) dipolar [105], (b) dipolar-quadrupolar [34] or (c) quadrupolar [106] particle&defect units. (d) Assembly entangled with a knotted disclination loop [93]. (e) Three-dimensional nematic colloidal crystal assembled with laser tweezers, with (right) a 3D confocal image [35].

structures emerge with distinct spatially varying nematic profiles, which can also include topological defects of various types and topological invariants, such as disclinations, points defects, and umbilic defects. More generally, fluidity of nematics can have important consequences in applications, such as in of liquid crystal displays [54, 55], or it can lead to complex pattern formation, as for example in the process of electroconvection [57, 124]. Rheological properties have been studied for variety of liquid crystalline materials, ranging from thermotropic liquid crystals [71] to cholesterics [125] and suspensions of viruses [126]. A major recent interest is in the development of nematic microfluidic concepts to active nematic systems [58].

A. Porous nematic microfluidics for generation of umbilic defect structures

Umbilic defects are observed to emerge when the nematic is pushed along the porous microchannels with all surfaces imposing uniform planar anchoring *along* the direction of the channel (see Fig. 7) [127]. The porous channels are set up as rectangular micro-channels with inserted cylindrical barriers, e.g. visualise long cylindrical fibres immersed in the channels. The porous barriers change the effective landscape of the microfluidic channel by introducing geometrical pores of various shapes and sizes, which cause the flow velocity to obtain multiple flow peaks and flow saddle points and it is the local flow peaks and saddles which generate the umbilic defects via the backflow mechanism. Director field in the umbilic defect is tilted towards its core and is consequently continuous everywhere in space. A notable difference between regular singular defects in liquid crystals and umbilic defects is that half integer (winding number) defect lines can occur in disclinations, but not in umbilic defects lines.

Figure 7 (a, b, c, d) shows the rectangular microfluidic channel with inserted cylindrical barriers of different-thickness and arranged in different lattices. Figure 7 (a, b) shows the microchannel with triangular lattice of barriers where depending on the barrier radius, we observe formation of two different lattices of the umbilic defects. In thin barrier regime, +1 umbilics form triangular lattice and -1 umbilics a square lattice. However, if the barriers are thick compared to the interspaces between them, +1 umbilics form hexagonal lattice and -1 umbilics arrange into a Kagome lattice. Both types of umbilic defects in porous microchannel with square lattice of barriers (Fig. 7 c)

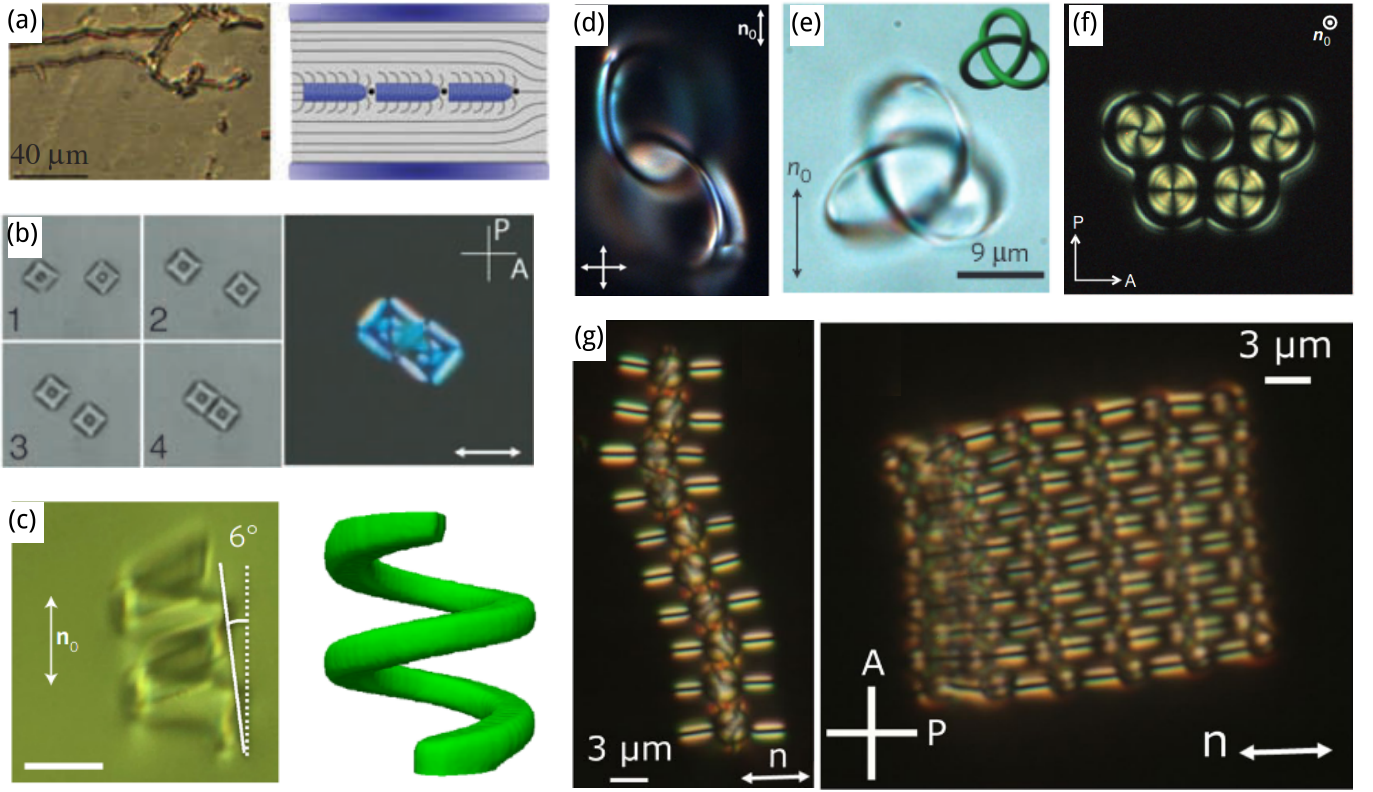


FIG. 6: Nematic colloids with different particle shapes. Structures show own assembly characteristics, mediated by both the defects and the elastic deformation of the director field. Geometry and topology of the particles play a strong role in the behaviour of the nematic host, and can be tuned to achieve desired goals. Sources: (a): [119], (b): [113], (c) [117], (e): [112], (d): [48] (f): [47] (g): [110].

form lattices of the same symmetry. If the barriers are arranged into a hexagonal lattice (Fig. 7 d) umbilic defects of strength $+1$ form triangular and -1 umbilics a Kagome lattice.

In such channels, the deformation of the director field is a result of competition between the surface alignment imposed by the channel surfaces and the flow shear, where the flow shear turns the director away from the direction imposed by the surfaces. A local maximum in the flow field yields an umbilic defect of positive strength and a saddle point gives an umbilic defect of negative strength. Actually, by designing flow profiles with different symmetry beyond simple peaks and horse saddles, umbilic defects of higher umbilic strength can be created. Indeed, a peak in the velocity field generates a $+1$ umbilic and a horse saddle a -1 umbilic. But two peaks without a saddle point (a minimum and a maximum) generate umbilic of strength $+2$, whereas a three-valley saddle (monkey saddle) and a four-valley saddle yield umbilics of strength -2 and -3 , respectively (see Fig. 7 e).

To generalise the results, the mutual – backflow – coupling between the flow field and nematic orientational ordering is shown as an interesting way for creating birefringent defect lattices in complex fluids via direct microfluidic approach. By controlling the symmetry and size of the porous barriers in the channels, one can design various umbilic arrangements and lattices ranging from simple square, to triangular and even Kagome. As objects, the umbilic defects are inherently birefringent and could be used for manipulating the flow of light at various levels and frequency scales, or used as switchable and controllable objects for trapping and guiding inclusions – such as colloidal particles –, relevant in microtransport and mixing applications.

B. Stationary singular defect structures in junctions of nematic microfluidic channels

Complex flow field profiles in nematic microchannels can be used to create nematic microstructures with *singular* topological defects, such as disclinations, defect loops, or topological points defects. Typically, singular defects emerge in microfluidic geometries, where surfaces impose perpendicular (or tilted, but not inplane) surface alignment, such as in microfluidic channels with homeotropic anchoring, where energetic competition between escaped and singular

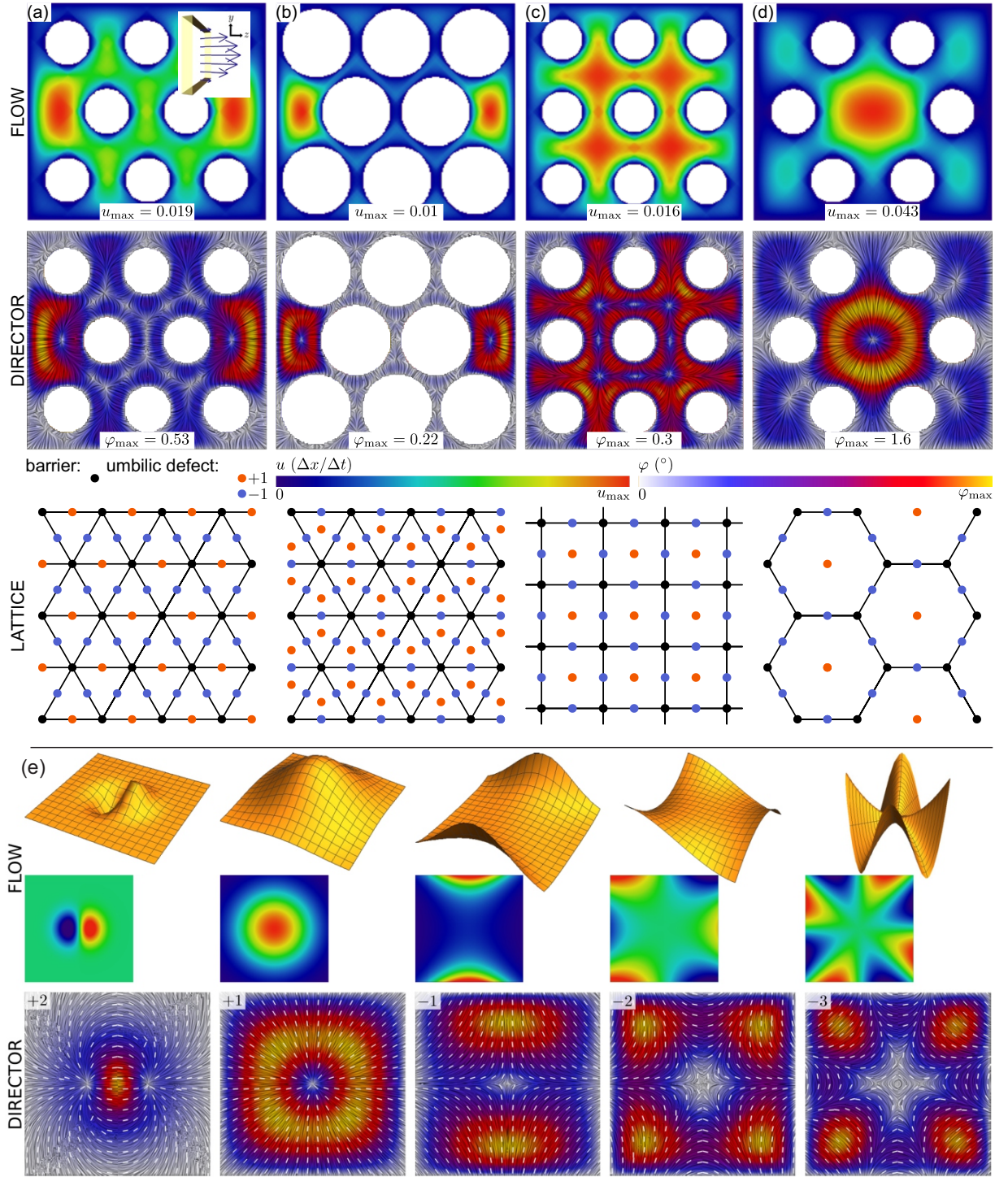


FIG. 7: Porous nematic microfluidics as generator for umbilic defect lattice structures. Porous microchannels with cylindrical barriers are arranged into (a) and (b) triangular, (c) square, and (d) hexagonal lattices, creating: in (a) triangular lattice of +1 umbilics and a rectangular lattice of -1 umbilics form, in (b) hexagonal lattice of +1 umbilics and a Kagome lattice of -1 umbilics, in (c) square lattice of both +1 and -1 umbilics, and in (d) triangular lattice of +1 umbilics and Kagome lattice of -1 umbilic. The bottom panels show generalization of the observed structures. (e) Generation of umbilic defects of variable (high) umbilic strength by flow peaks and flow saddle points. A local peak in the velocity field generates a + umbilic and flow saddle generates a - umbilic. Adapted from [127].

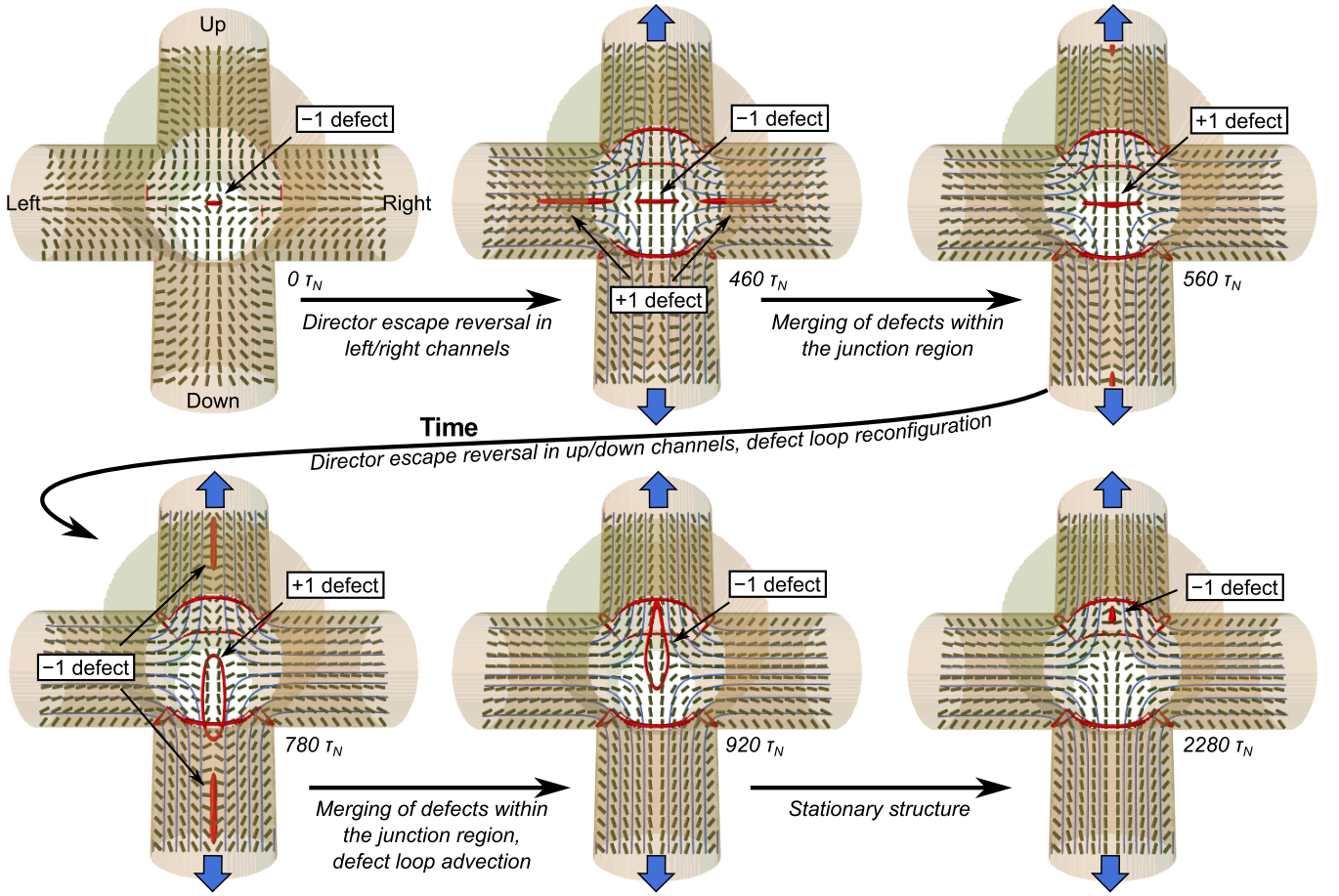


FIG. 8: Flow stabilised structures in junctions of nematic-filled channels. Defect dynamics is shown in a junction with extensile flow (i.e. two outlet channels indicated by two blue arrows, and four inlet channels). Initial director profile has 2 outward escaping profiles and 4 inward escaping equilibrium configurations with a -1 defect at the channel junction centre. Flow direction in top and bottom channels is aligned with the direction of director escape. As the nematic undergoes a flow-aligning transition in the left and right channel, a pair of $+1$ defects is created at open channel boundaries. The pair coalesces with the previously residing -1 defect, forming a $+1$ defect and thus preserving the bulk topological charge. Similarly, undergoing a flow alignment transition, -1 defects are created in the up and in the down channel. The defects interact and form a stationary state, consisting of a single -1 bulk defect, which is displaced from the centre of the junction in the direction of one of the outgoing flows. Time is measured in units of nematic characteristic time scale $\tau_N = \frac{\xi_N^2}{\Gamma L}$. Adapted from [128].

profiles lead to diverse microfluidic structures. For example, in [129] junctions of 4, 6, and 8 microchannels (treated for homeotropic anchoring) are used to create nematic defects with different topological charge. The main mechanism for the creation of such singular defects is the fact that in the centre of a nematic microchannel at sufficiently large Ericksen numbers, the director turns along the channel. Actually, in nematic microfluidics two topological structures can be present, i.e. the topological defects in the orientational field of the nematic and the stagnation points in the velocity field, which more generally, is an example of a cross-talk between topological structures of different fields.

Nematic structures in microfluidic environments are of particular interest due to their memory effects and switching possibilities, providing a route towards new optic and photonic materials [16, 40, 41, 130]. In Fig. 8 we show flow-induced dynamics of a defect structure inside a junction of six cylindrical capillaries. In a cylindrical confinement with homeotropic anchoring and without flow, nematic director prefers the escaped alignment, in which case the director in the middle of the channel points along the channel direction. This leads to a variety of equilibrium structures, depending on the direction of the director escape in individual channels [41]. One of such structures is shown in the first snapshot of Fig. 8, where a -1 topological defect resides in the centre of the junction. Preferred nematic alignment in a capillary when flow is switched on is with the direction of the director escape along the flow. This leads to the flow-induced reconfiguration of the defect structure in a microjunction (Fig. 8). Upon the director escape reversal in left and right channel two $+1$ defects are created. They merge with the -1 defect in the junction centre,

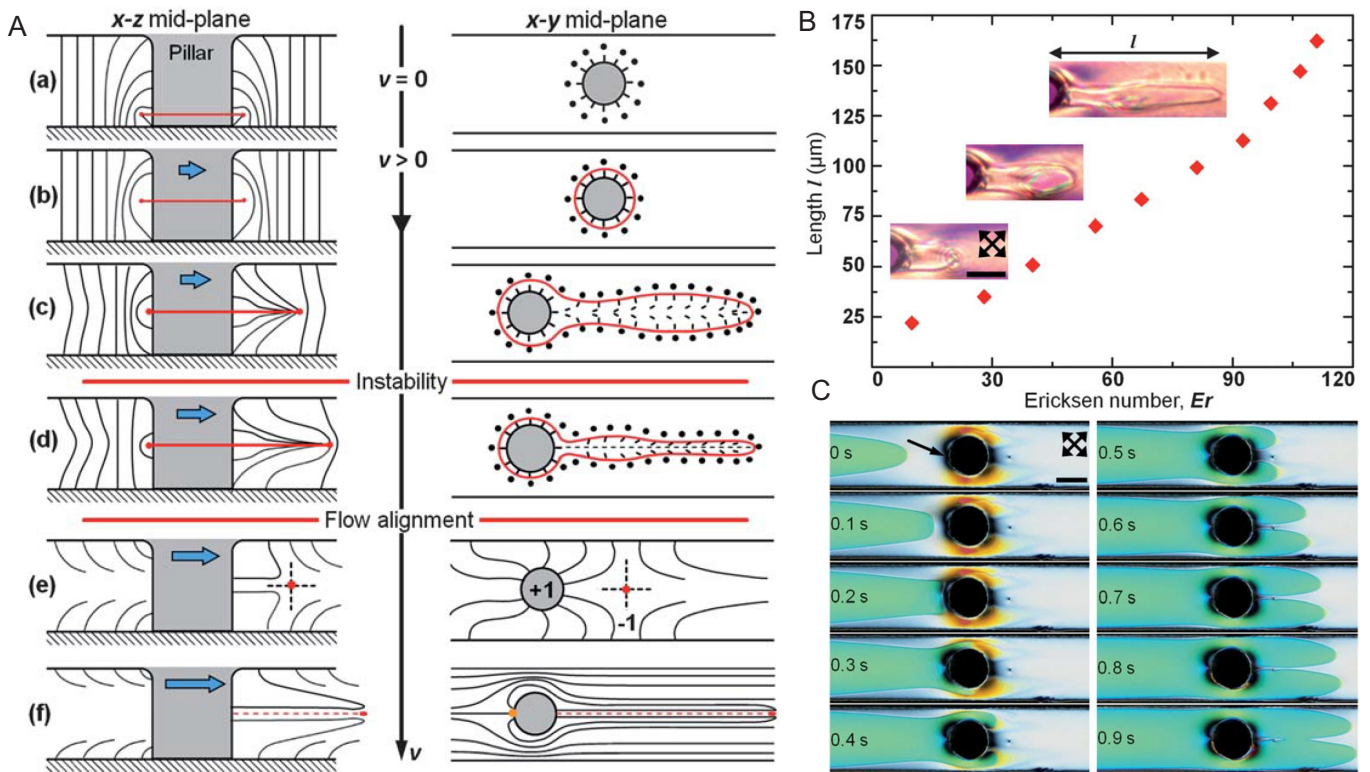


FIG. 9: Nematic flow past a cylindrical barrier in nematic microchannel. (A) Morphological evolution of the defect structures in the presence of flow. Defects are drawn in red; black lines show the corresponding director. (B) Extension of the singular loop (measured between the pillar center and the leading end of the defect) shows a non-linear dependence with the Ericksen number Er . Insets show extension of the semi-integer defect loop with increasing the flow speed, observed between crossed-polarizers. Scale bar: 50 μm . (C) Time sequence of polarized micrographs representing the flow-alignment of the nematic director in microchannel. A distinct birefringent domain (green in appearance) with a parabolic boundary is observed upstream of the micro-pillar. Adapted from [131].

forming a defect structure with topological charge of $+1$. Similar process is repeated as a -1 defect is created in the up and in the down channel which merge with the preexisting $+1$ defect, leading to the formation of a -1 defect in the junction. The position of the defect is slightly off-centre since it is advected by the flow. Depending on the geometry of the initial equilibrium structure and the arrangement of the flow towards and away from the junction, a variety of switching processes and flow-stabilised structures is possible [128]. This example shows how porous networks with microfluidic functionality can be turned into advanced platform for generation of various topological nematic field structures.

C. Nematic flow past microfluidic obstacles

While flow might lead to the formation of stationary nematic structures, unstable temporal behaviour might also emerge. This was observed in the case of nematic flowing past an obstacle in a shape of a pillar within a microchannel [131] (see Fig. 9). In equilibrium, homeotropic anchoring conditions on the surface of the pillar and on the edges of the microchannel induce a defect loop surrounding the pillar. At low flow rates the defect loop aligns in the middle of the channel and stretches along the flow. At even higher flow magnitudes a flow aligning transition is reached, after which sufficiently far away from the micropillar, the director in the centre of the channel points along the channel and not perpendicular to it. This leads to the formation of a -1 point defect, which is separated from the pillar by a wall like region of high distortion. After the creation of the -1 defect, the length of the wall structure increases in time due to strong velocity field, causing an instability, in which a pair of ± 1 defects is created in the wall. This event splits the wall in two. The part of the wall that is further along the flow consist of a $+1$ and a -1 defect with no net topological charge and is annihilated. The part of the wall closer to the pillar gradually grows until the splitting event is repeated.

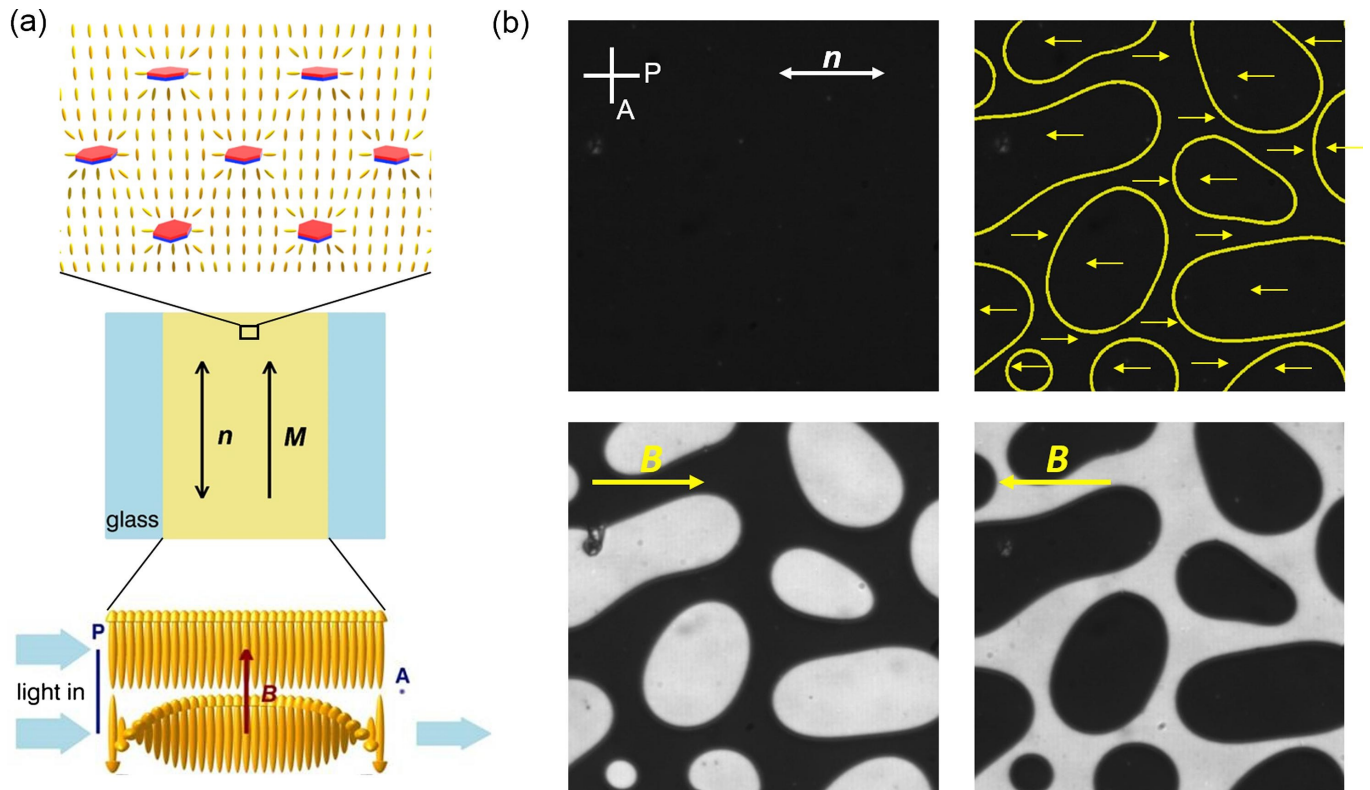


FIG. 10: Ferromagnetic suspension of Ba hexaferrite nanoplates in NLC: (a) Magnetic nanoplates (red and blue) orient with their magnetic moments along the average order of liquid-crystal molecules (yellow ellipsoids). (b) Polarized-light microscopy images of two types of antiparallel magnetic domains form with the magnetization along the NLC orientation (denoted by n). P and A indicate the orientation of the polarizer and analyser, respectively. The upper images show the suspension in the absence of the field; on the right-hand-side image the domain walls are drawn. The bottom images show the response of the domains to a magnetic field. Adapted from [134].

The nematic microfluidic setups can be further advanced by using microchannels with structured walls, such as in Ref. [132], where nematodynamic concepts are used for manipulation and transport of colloidal particles. Using wavy walls of microfluidic cells and channels, the authors are able to realise tunable colloid trajectories, leading to distinct particle docking and lock-and-key interactions. The interactions are based on the design of the alternating splay and bend distortions, which define a smoothly varying elastic energy profile. These approaches of transport and microflow manipulation can be further complemented by applying external mechanical, electric and light fields, such as in [133], where driving pressure can be used to stabilize and manipulate distinct topologically protected intermediate states. More generally, nematofluidic setups in combination with external stimuli and fields, enables to induce different flow state transitions on demand through channel geometry, application of laser tweezers, and control of the flow rate/pressure.

VI. FERROMAGNETIC LIQUID CRYSTAL STRUCTURES

Design and different functionalisation of liquid crystal agents – from molecules to colloidal-type particles – can lead to realisation of different liquid crystal structures and even new liquid crystal phases. Distinct type of functionalisation is the development of ferromagnetic liquid crystal structures [20, 51], either in diluted or dense suspensions, which leads to combined effects of liquid crystal ordering and ferromagnetism. Effectively, such systems perform as liquid ferromagnets.

A. Suspensions of magnetic platelets in liquid crystals

A ferromagnetic nematic colloidal suspension was realised, as based on nanosized thin ferromagnetic colloidal platelets immersed in nematic liquid crystal [51]. The surfaces of the platelets are functionalised to impose perpendicular (homeotropic) alignment of the nematic, causing a stable nematic suspension with macroscopic spontaneous magnetization along the nematic director. Upon quenching of the suspension from the isotropic phase, the ferromagnetic domains form, which can be aligned upon cooling into monodomains by applying external magnetic fields. The material is an intriguing liquid that possesses two order parameters - i.e. the nematic director and magnetisation - which are mutually coupled. The aggregation of the ferromagnetic platelets is prevented by the nematic mediated elastic interactions between the platelets. More generally, this work is a demonstration of a novel multi ferroic material, and contributes to the development in the general field of anisotropic magnetic nanoparticle materials [134].

B. Dense suspensions of magnetic platelets in isotropic fluids

Colloidal fluid with ferromagnetic building blocks that at sufficiently high concentration exhibit liquid crystal ordering (i.e. without liquid crystal host, as in Section VIA) is realised to perform as liquid ferromagnets in the work led by N. A. Clark [20]. Distinctly, ferromagnetism in colloidal fluids is achieved by creating stable, fluid suspensions of well-dispersed magnetic nanoparticles in isotropic solvent, and further designing their mutual interactions to produce equilibrium, zero-field magnetization. In the work by Clark et al, barium hexaferrite (BF) nanoplates were suspended in isotropic n-butanol and surfactant-stabilized to produce a system of functionalized nanoplates with weak electrostatic repulsion, strong and anisotropic steric repulsion and magnetic interaction. Introducing the electrostatic repulsion prevented nanoparticle aggregation and enabled stable suspensions at essentially any concentration, importantly including at high volume fractions where spontaneous LC ordering of the platelets can emerge. The demonstrated nematic liquid crystal colloidal fluid is distinctly ferromagnetic, also forming birefringent interfacial spikes at the isotropic -nematic ferromagnet interface upon applying external magnetic field perpendicular to the interface. Finally, the realised ferromagnetic fluid produces distinctive magnetic self-interaction effects, such as fluid block domains arranged in closed flux loops, and makes this material highly sensitive, even in the Earth's magnetic field.

VII. CONCLUSIONS

Nematic fluids are characterised by the orientational order of their building blocks and include different materials, from molecular fluids, colloidal liquid crystals to viruses. The nematic orientational order is soft and responsive as an effective elastic medium to external stimuli, including mechanical fields, pressure, light, electric & magnetic fields, and dispersed colloidal particles. The strong susceptibility to external stimuli makes nematic fluids potent materials in systems that require controllability and tuneability, which is today extensively used in display and optical applications, with strong development also towards photonics and metamaterial applications.

This brief review points out three selected directions for realising liquid crystal structures - nematic colloids, nematic microfluidics and ferromagnetic liquid crystal structures. All these topics fundamentally use the distinct liquid crystal ordering and its manipulation, either through the composition/structure of the actual materials or through the external fields or frustration, to produce novel material behaviour or material mechanisms. This complex soft matter naturally reaches towards other field of science and technology, notably including optics and photonics, biological and active matter, topology, microfluidics and fluid dynamics, sensing and metamaterials.

Finally, Noel A. Clark is one of the world pioneers who contributed and is still shaping this field of complex and functional soft matter and its applications with his profound ingenuity and wisdom.

VIII. ACKNOWLEDGEMENTS

Authors acknowledge funding from Slovenian Research Agency (ARRS) contracts P1-0099, J1-1697, J1-2462 and N1-0195. MR acknowledges funding from ERC Advanced grant LOGOS.

[1] F. C. Frank. I. Liquid crystals. On the theory of liquid crystals. *Discuss. Faraday Soc.*, 25:19, 1958.

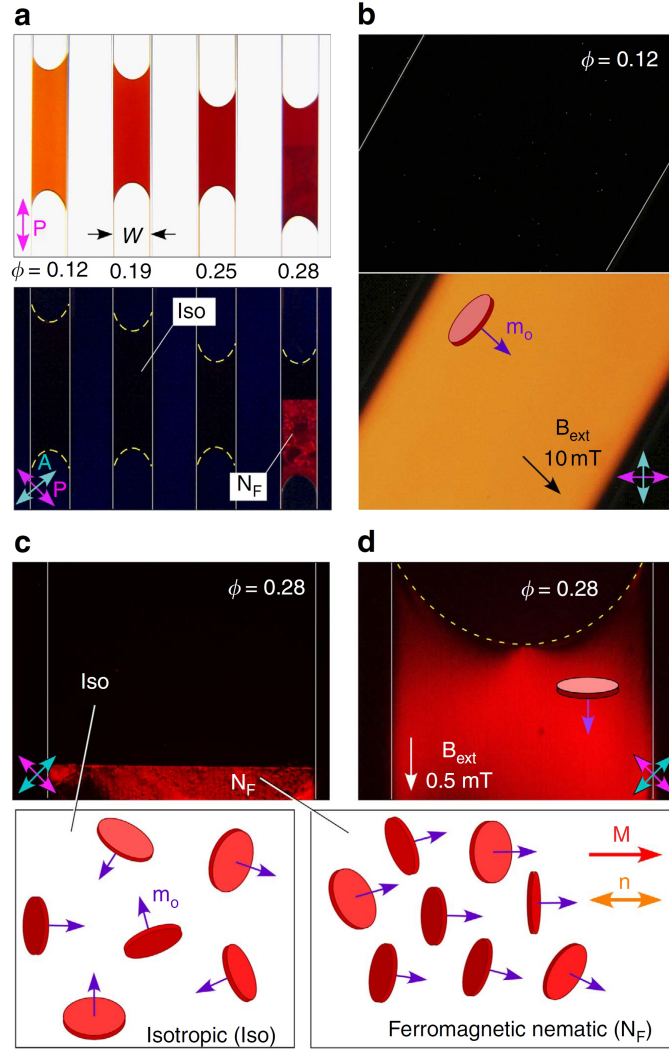


FIG. 11: Nematic ferrofluid from suspension of barium ferrite nanoplatelets in n-butanol. (a) Nanoplatelet suspensions viewed in transmitted light with optical polarization conditions indicated (Polarizer: magenta, P; analyser: cyan, A). Low-volume fraction suspensions are isotropic (Iso), appearing dark between crossed polarizers. The orange/red colour is due to optical absorption by the nanoplatelets. At higher concentrations ($\phi \gtrsim 0.28$), a birefringent ferromagnetic nematic (NF) phase appears in the lower part of the cell. (b) An applied in-plane magnetic field induces birefringence in the isotropic phase, with the principal axes of the optical dielectric tensor along and normal to external magnetic field and the induced macroscopic magnetization density parallel to external magnetic field. (c) The NF phase is separated gravitationally from the isotropic region by a sharp, horizontal interface. Equilibrium Iso and NF structures deduced from birefringence and dichroism measurements are illustrated. (d) The Iso phase is magnetized and the Iso–NF interface becomes continuous under applied magnetic field. Samples are sealed in rectangular glass capillaries. The boundaries of the cells are indicated by the solid thin white lines and the air–liquid interfaces by the dashed yellow lines. Adapted from [20].

- [2] W. Maier and A. Saupe. Eine einfache molekulare Theorie des nematischen kristallinflüssigen Zustandes. *Z. Naturforsch.*, 13:564–566, 1958.
- [3] W. Maier and A. Saupe. Eine einfache molekular-statistische Theorie der nematischen kristallinflüssigen Phase. Teil I. *Z. Naturforsch.*, 14:882–889, 1959.
- [4] W. Maier and A. Saupe. Eine einfache molekular-statistische Theorie der nematischen kristallinflüssigen Phase. Teil II. *Z. Naturforsch.*, 15:287–292, 1960.
- [5] P. G. De Gennes. Short Range Order Effects in the Isotropic Phase of Nematics and Cholesterics. *Mol. Cryst. Liq. Cryst.*, 12:193, 1971.
- [6] W Helfrich and M. Schadt, 1970. Swiss patent NO133857C.
- [7] J. Fergason, 1971. US patent US3731986A.
- [8] Haiwei Chen and Shin-Tson Wu. Advanced liquid crystal displays with supreme image qualities. *Liquid Crystals Today*, 28:4, 2019.

- [9] T. W. Stinson, J. D. Litster, and N. A. Clark. Static and Dynamic Behavior near the Order Disorder Transition of Nematic Liquid Crystals. *J. Phys. Colloques*, 33:C1–69, 1972.
- [10] Charles Y. Young, Ronald Pindak, Noel A. Clark, and Robert B. Meyer. Light-scattering Study of Two-Dimensional Molecular-Orientation Fluctuations in a Freely Suspended Ferroelectric Liquid-Crystal Film. *Phys. Rev. Lett.*, 40:773, 1978.
- [11] Noel A. Clark and Sven T. Lagerwall. Submicrosecond bistable electro-optic switching in liquid crystals. *Appl. Phys. Lett.*, 36:899, 1980.
- [12] Noel A. Clark and Sven T. Lagerwall, 1980. US patent Patent US4367924A.
- [13] C. R. Safinya, D. Roux, G. S. Smith, S. K. Sinha, P. Dimon, N. A. Clark, and A. M. Bellocq. Steric Interactions in a Model Multimembrane System: A Synchrotron X-Ray Study. *Phys. Rev. Lett.*, 57:2718, 1986.
- [14] Tommaso Bellini, Noel Clark, Chris Muzny, Lei Wu, Carl Garland, Dale Schaefer, and Bernard Oliver. Phase behavior of the liquid crystal 8cb in a silica aerogel. *Phys. Rev. Lett.*, 69:788, 1992.
- [15] Darren R. Link, Renfan Shao, Giorgio Natale, Joseph E. MacLennan, Noel A. Clark, Eva Körblová, and David M. Walba. Spontaneous Formation of Macroscopic Chiral Domains in a Fluid Smectic Phase of Achiral Molecules. *Science*, 278:1924, 1997.
- [16] Daeseung Kang, Joseph MacLennan, Noel Clark, Anvar Zakhidov, and Ray Baughman. Electro-optic behavior of liquid-crystal-filled silica opal photonic crystals: Effect of liquid-crystal alignment. *Phys. Rev. Lett.*, 86:4052, 2001.
- [17] M. Nakata, G. Zanchetta, B. D. Chapman, C. D. Jones, J. O. Cross, R. Pindak, T. Bellini, and N. A. Clark. End-to-end Stacking and Liquid Crystal Condensation of 6- to 20-base Pair DNA Duplexes. *Science*, 318:1276, 2007.
- [18] L. E. Hough, H. T. Jung, D. Krüerke, M. S. Heberling, M. Nakata, C. D. Jones, D. Chen, D. R. Link, J. Zasadzinski, G. Heppke, J. P. Rabe, W. Stocker, E. Körblová, D. M. Walba, M. A. Glaser, and N. A. Clark. Helical Nanofilament Phases. *Science*, 325:456, 2009.
- [19] D. Chen, J. H. Porada, J. B. Hooper, A. Klittnick, Y. Shen, M. R. Tuchband, E. Korblová, D. Bedrov, D. M. Walba, M. A. Glaser, J. E. MacLennan, and N. A. Clark. Chiral heliconical ground state of nanoscale pitch in a nematic liquid crystal of achiral molecular dimers. *Proc. Natl. Acad. Sci.*, 110:15931, 2013.
- [20] M. Shuai, A. Klittnick, Y. Shen, G. P. Smith, M. R. Tuchband, C. Zhu, R. G. Petschek, A. Mertelj, D. Lisjak, M. Čopič, J. E. MacLennan, M. A. Glaser, and N. A. Clark. Spontaneous liquid crystal and ferromagnetic ordering of colloidal magnetic nanoplates. *Nat. Commun.*, 7:10394, 2016.
- [21] M. Kléman. Defect densities in directional media, mainly liquid crystals. *Philos. Mag.*, 27:1057, 1973.
- [22] G. E. Volovik and V. P. Mineev. Investigation of singularities in superfluid He3 in liquid crystals by the homotopic topology methods. *J. Exp. Theor. Phys.*, 45:1186, 1977.
- [23] N. Mermin. The topological theory of defects in ordered media. *Rev. Mod. Phys.*, 51:591, 1979.
- [24] G.E. Volovik and O.D. Lavrentovich. Topological dynamics of defects: boojums in nematic drops. *Zh. Eksp. Teor. Fiz.*, 85:1159, 1983.
- [25] J. W. Doane, N. A. Vaz, B.-G. Wu, and S. Žumer. Field controlled light scattering from nematic microdroplets. *Appl. Phys. Lett.*, 48:269, 1986.
- [26] Mikhail V Kurik and O D Lavrentovich. Defects in liquid crystals: homotopy theory and experimental studies. *Sov. Phys. Usp.*, 31:196, 1988.
- [27] G Crawford, D Allender, and J Doane. Surface elastic and molecular-anchoring properties of nematic liquid crystals confined to cylindrical cavities. *Phys. Rev. A*, 45:8693, 1992.
- [28] E. Terentjev. Disclination loops, standing alone and around solid particles, in nematic liquid crystals. *Phys. Rev. E*, 51:1330, 1995.
- [29] Philippe Poulin, Holger Stark, T. C. Lubensky, and D. A. Weitz. Novel Colloidal Interactions in Anisotropic Fluids. *Science*, 275:1770, 1997.
- [30] T. C. Lubensky, David Pettey, Nathan Currier, and Holger Stark. Topological defects and interactions in nematic emulsions. *Phys. Rev. E*, 57:610, 1998.
- [31] Holger Stark. Physics of colloidal dispersions in nematic liquid crystals. *Phys. Rep.*, 351:387, 2001.
- [32] J. Fukuda and H. Yokoyama. Director configuration and dynamics of a nematic liquid crystal around a two-dimensional spherical particle: Numerical analysis using adaptive grids. *Eur. Phys. J. E*, 4:389, 2001.
- [33] Igor Mušević, Miha Škarabot, Uroš Tkalec, Miha Ravnik, and Slobodan Žumer. Two-dimensional Nematic Colloidal Crystals Self-Assembled by Topological Defects. *Science*, 313:954, 2006.
- [34] U. Ognysta, A. Nych, V. Nazarenko, M. Škarabot, and I. Mušević. Design of 2d Binary Colloidal Crystals in a Nematic Liquid Crystal. *Langmuir*, 25:12092, 2009.
- [35] A. Nych, U. Ognysta, M. Škarabot, M. Ravnik, S. Žumer, and I. Mušević. Assembly and control of 3d nematic dipolar colloidal crystals. *Nat. Commun.*, 4:1489, 2013.
- [36] Yimin Luo, Francesca Serra, Daniel A. Beller, Mohamed A. Gharbi, Ningwei Li, Shu Yang, Randall D. Kamien, and Kathleen J. Stebe. Around the corner: Colloidal assembly and wiring in groovy nematic cells. *Phys. Rev. E*, 93:032705, 2016.
- [37] M. Ravnik, M. Škarabot, S. Žumer, U. Tkalec, I. Poberaj, D. Babič, N. Osterman, and I. Mušević. Entangled Nematic Colloidal Dimers and Wires. *Phys. Rev. Lett.*, 99:247801, 2007.
- [38] Simon Čopar and Slobodan Žumer. Nematic Braids: Topological Invariants and Rewiring of Disclinations. *Phys. Rev. Lett.*, 106:177801, 2011.
- [39] U. Tkalec, M. Ravnik, S. Čopar, S. Žumer, and I. Mušević. Reconfigurable Knots and Links in Chiral Nematic Colloids. *Science*, 333:62, 2011.

- [40] Takeaki Araki, Marco Buscaglia, Tommaso Bellini, and Hajime Tanaka. Memory and topological frustration in nematic liquid crystals confined in porous materials. *Nat. Mater.*, 10:303, 2011.
- [41] Francesca Serra, Krishna C. Vishnubhatla, Marco Buscaglia, Roberto Cerbino, Roberto Osellame, Giulio Cerullo, and Tommaso Bellini. Topological defects of nematic liquid crystals confined in porous networks. *Soft Matter*, 7:10945, 2011.
- [42] Simon Čopar, Noel A. Clark, Miha Ravnik, and Slobodan Žumer. Elementary building blocks of nematic disclination networks in densely packed 3d colloidal lattices. *Soft Matter*, 9:8203, 2013.
- [43] C. P. Lapointe, T. G. Mason, and I. I. Smalyukh. Shape-controlled Colloidal Interactions in Nematic Liquid Crystals. *Science*, 326:1083, 2009.
- [44] J Dontabhaktuni, M Ravnik, and S Žumer. Quasicrystalline tilings with nematic colloidal platelets. *Proc. Natl. Acad. Sci.*, 111:2464, 2014.
- [45] Maryam Nikkhou, Miha Škarabot, Simon Čopar, Miha Ravnik, Slobodan Žumer, and Igor Mušević. Light-controlled topological charge in a nematic liquid crystal. *Nat. Phys.*, 11:183, 2015.
- [46] H. Mundoor, B. Senyuk, and I. I. Smalyukh. Triclinic nematic colloidal crystals from competing elastic and electrostatic interactions. *Science*, 352:69, 2016.
- [47] Bohdan Senyuk, Qingkun Liu, Sailing He, Randall D. Kamien, Robert B. Kusner, Tom C. Lubensky, and Ivan I. Smalyukh. Topological colloids. *Nature*, 493:200, 2013.
- [48] Angel Martinez, Miha Ravnik, Brice Lucero, Rayshan Visvanathan, Slobodan Žumer, and Ivan I. Smalyukh. Mutually tangled colloidal knots and induced defect loops in nematic fields. *Nat. Mater.*, 13:258, 2014.
- [49] Miha Ravnik, Simon Čopar, and Slobodan Žumer. Particles with changeable topology in nematic colloids. *J. Phys.: Condens. Matter*, 27:354111, 2015.
- [50] Ye Yuan, Mykola Tasinkevych, and Ivan I. Smalyukh. Colloidal interactions and unusual crystallization versus de-mixing of elastic multipoles formed by gold mesoflowers. *Nat. Commun.*, 11:811, 2020.
- [51] Alenka Mertelj, Darja Lisjak, Miha Drofenik, and Martin Čopič. Ferromagnetism in suspensions of magnetic platelets in liquid crystal. *Nature*, 504:237, 2013.
- [52] J. L. Ericksen. Anisotropic fluids. *Arch. Rational Mech. Anal.*, 4:231, 1959.
- [53] F.M. Leslie. Theory of Flow Phenomena in Liquid Crystals. *Advances in Liquid Crystals*, 4:1–81, 1979.
- [54] Dwight W Berreman. Liquid-crystal twist cell dynamics with backflow. *J. Appl. Phys.*, 46:3746, 1975.
- [55] C Z van Doorn. Dynamic behavior of twisted nematic liquid-crystal layers in switched fields. *J. Appl. Phys.*, 46:3738, 1975.
- [56] L Kramer and W Pesch. Convection Instabilities in Nematic Liquid Crystals. *Annu. Rev. Fluid Mech.*, 27:515, 1995.
- [57] N. Éber, P. Salamon, and Á. Buka. Electrically induced patterns in nematics and how to avoid them. *Liquid Crystals Reviews*, 4:101, 2016.
- [58] Amin Doostmohammadi, Tyler N. Shendruk, Kristian Thijssen, and Julia M. Yeomans. Onset of meso-scale turbulence in active nematics. *Nat. Commun.*, 8:15326, 2017.
- [59] Anupam Sengupta. Topological microfluidics: present and prospects. *Liquid Crystals Today*, 24:70, 2015.
- [60] P G de Gennes and J Prost. *Physics of Liquid Crystals*. Oxford University Press, New York, 1993.
- [61] K Schiele and S Trimper. On the {Elastic} {Constants} of a {Nematic} {Liquid} {Crystal}. *phys. stat. sol.*, 118:267, 1983.
- [62] Miha Ravnik and Slobodan Žumer. Landau–de Gennes modelling of nematic liquid crystal colloids. *Liq. Cryst.*, 36:1201, 2009.
- [63] Daniel M. Sussman and Daniel A. Beller. Fast, Scalable, and Interactive Software for Landau-de Gennes Numerical Modeling of Nematic Topological Defects. *Front. Phys.*, 7:273, 2019.
- [64] Jeffrey C. Everts and Miha Ravnik. Ionically Charged Topological Defects in Nematic Fluids. *Phys. Rev. X*, 11:011054, 2021.
- [65] A N Beris and B J Edwards. *Thermodynamics of Flowing Systems with Internal Microstructure*. Oxford University Press, New York, 1994.
- [66] Tiezheng Qian and Ping Sheng. Generalized hydrodynamic equations for nematic liquid crystals. *Phys. Rev. E*, 58:7475, 1998.
- [67] Colin Denniston, Enzo Orlandini, and J Yeomans. Lattice {Boltzmann} simulations of liquid crystal hydrodynamics. *Phys. Rev. E*, 63:56702, 2001.
- [68] Ž Kos, J Aplinc, U Mur, and M Ravnik. *Mesoscopic Approach to Nematic Fluids in Flowing Matter (Eds. F. Toschi and M. Sega)*. Springer Open, 2019.
- [69] D Svenšek and S Žumer. Hydrodynamics of pair-annihilating disclination lines in nematic liquid crystals. *Phys. Rev. E*, 66:21712, 2002.
- [70] Géza Tóth, Colin Denniston, and J M Yeomans. Hydrodynamics of {Topological} {Defects} in {Nematic} {Liquid} {Crystals}. *Phys. Rev. Lett.*, 88:105504, 2002.
- [71] Anupam Sengupta, Uroš Tkalec, Miha Ravnik, Julia Yeomans, Christian Bahr, and Stephan Herminghaus. Liquid {Crystal} {Microfluidics} for {Tunable} {Flow} {Shaping}. *Phys. Rev. Lett.*, 110:48303, 2013.
- [72] C. Denniston, D. Marenduzzo, E. Orlandini, and J.M. Yeomans. Lattice Boltzmann algorithm for three-dimensional liquid-crystal hydrodynamics. *Phil. Trans. R. Soc. A*, 362:1745, 2004.
- [73] M E Cates, K Stratford, R Adhikari, P Stansell, J-C Desplat, I Pagonabarraga, and A J Wagner. Simulating colloid hydrodynamics with lattice Boltzmann methods. *J. Phys.: Condens. Matter*, 16:S3903, 2004.
- [74] R. James, E. Willman, F.A. FernandezFernandez, and S.E. Day. Finite-element modeling of liquid-crystal hydrodynamics

- with a variable degree of order. *IEEE Trans. Electron Devices*, 53:1575, 2006.
- [75] Shubhadeep Mandal and Marco G. Mazza. Multiparticle collision dynamics for tensorial nematodynamics. *Phys. Rev. E*, 99:89, 2019.
 - [76] Tyler N. Shendruk and Julia M. Yeomans. Multi-particle collision dynamics algorithm for nematic fluids. *Soft Matter*, 11:5101, 2015.
 - [77] M. Kléman, L. Michel, and G. Toulouse. Classification of topologically stable defects in ordered media. *J. Phys. Lett. Paris*, 38:195, 1977.
 - [78] M. Kleman. Defects in liquid crystals. *Rep. Prog. Phys.*, 52:555, 1989.
 - [79] Sriram Ramaswamy, Rajaram Nityananda, V. A. Raghunathan, and Jacques Prost. Power-law Forces Between Particles in a Nematic. *Mol. Cryst. Liq. Crys. A*, 288:175, 1996.
 - [80] O. D. Lavrentovich. Topological defects in dispersed liquid crystals, or words and worlds around liquid crystal drops. *Liq. Cryst.*, 24:117, 1998.
 - [81] David Seč, Simon Čopar, and Slobodan Žumer. Topological zoo of free-standing knots in confined chiral nematic fluids. *Nat. Commun.*, 5:3057, 2014.
 - [82] Alexandre Darmon, Michael Benzaquen, Simon Čopar, Olivier Dauchot, and Teresa Lopez-Leon. Topological defects in cholesteric liquid crystal shells. *Soft Matter*, 12:9280, 2016.
 - [83] Gregor Posnjak, Simon Čopar, and Igor Muševič. Hidden topological constellations and polyvalent charges in chiral nematic droplets. *Nat. Commun.*, 8:14594, 2017.
 - [84] Joseph Pollard, Gregor Posnjak, Simon Čopar, Igor Muševič, and Gareth P. Alexander. Point Defects, Topological Chirality, and Singularity Theory in Cholesteric Liquid-Crystal Droplets. *Phys. Rev. X*, 9:1442, 2019.
 - [85] Klaus Janich. Topological properties of ordinary nematics in 3-space. *Acta Appl Math*, 8:65, 1987.
 - [86] Gareth P. Alexander, Bryan Gin ge Chen, Elisabetta A. Matsumoto, and Randall D. Kamien. Colloquium: Disclination loops, point defects, and all that in nematic liquid crystals. *Rev. Mod. Phys.*, 84:497, 2012.
 - [87] Simon Čopar. Topology and geometry of nematic braids. *Phys. Rep.*, 538:1, 2014.
 - [88] Thomas Machon and Gareth P. Alexander. Global defect topology in nematic liquid crystals. *Proc. R. Soc. A*, 472:20160265, 2016.
 - [89] S. Čopar and S. Žumer. Quaternions and hybrid nematic disclinations. *Proc. R. Soc. A*, 469:20130204, 2013.
 - [90] Jack Binysh, Žiga Kos, Simon Čopar, Miha Ravnik, and Gareth P. Alexander. Three-dimensional Active Defect Loops. *Phys. Rev. Lett.*, 124:257, 2020.
 - [91] Daniel A. Beller, Thomas Machon, Simon Čopar, Daniel M. Sussman, Gareth P. Alexander, Randall D. Kamien, and Ricardo A. Mosna. Geometry of the Cholesteric Phase. *Phys. Rev. X*, 4:031050, 2014.
 - [92] V. Poenaru and G. Toulouse. The crossing of defects in ordered media and the topology of 3-manifolds. *J. Phys.*, 38:887, 1977.
 - [93] Simon Čopar, Uroš Tkalec, Igor Muševič, and Slobodan Žumer. Knot theory realizations in nematic colloids. *Proc. Natl. Acad. Sci.*, 112:1675, 2015.
 - [94] Thomas Machon. The topology of knots and links in nematics. *Liquid Crystals Today*, 28:58, 2019.
 - [95] Takeaki Araki, Francesca Serra, and Hajime Tanaka. Defect science and engineering of liquid crystals under geometrical frustration. *Soft Matter*, 9:8107, 2013.
 - [96] Kathrin Sentker, Arda Yildirim, Milena Lippmann, Arne W. Zantop, Florian Bertram, Tommy Hofmann, Oliver H. Seeck, Andriy V. Kityk, Marco G. Mazza, Andreas Schönhals, and Patrick Huber. Self-assembly of liquid crystals in nanoporous solids for adaptive photonic metamaterials. *Nanoscale*, 11:23304, 2019.
 - [97] Youngwoo Yi, Giuseppe Lombardo, Neil Ashby, Riccardo Barberi, Joseph E. MacLennan, and Noel A. Clark. Topographic-pattern-induced homeotropic alignment of liquid crystals. *Phys. Rev. E*, 79:041701, 2009.
 - [98] Rebecca J. Carlton, Jacob T. Hunter, Daniel S. Miller, Reza Abbasi, Peter C. Mushenheim, Lie Na Tan, and Nicholas L. Abbott. Chemical and biological sensing using liquid crystals. *Liquid Crystals Reviews*, 1:29, 2013.
 - [99] Chloe C. Tartan, John J. Sandford O'Neill, Patrick S. Salter, Jure Aplinc, Martin J. Booth, Miha Ravnik, Stephen M. Morris, and Steve J. Elston. Read on Demand Images in Laser-Written Polymerizable Liquid Crystal Devices. *Adv. Opt. Mater.*, 6:1800515, 2018.
 - [100] Dae Seok Kim, Simon Čopar, Uroš Tkalec, and Dong Ki Yoon. Mosaics of topological defects in micropatterned liquid crystal textures. *Science Advances*, 4:eaau8064, 2018.
 - [101] MinSu Kim and Francesca Serra. Tunable Dynamic Topological Defect Pattern Formation in Nematic Liquid Crystals. *Adv. Opt. Mater.*, 8:1900991, 2020.
 - [102] I. Muševič. Nematic colloids, topology and photonics. *Phil. Trans. R. Soc. A*, 371:20120266, 2013.
 - [103] Uroš Tkalec and Igor Muševič. Topology of nematic liquid crystal colloids confined to two dimensions. *Soft Matter*, 9:8140, 2013.
 - [104] U. Ognysta, A. Nych, V. Nazarenko, I. Muševič, M. Škarabot, M. Ravnik, S. Žumer, I. Poberaj, and D. Babič. 2d Interactions and Binary Crystals of Dipolar and Quadrupolar Nematic Colloids. *Phys. Rev. Lett.*, 100:217803, 2008.
 - [105] V. S. R. Jampani, M. Škarabot, M. Ravnik, S. Čopar, S. Žumer, and I. Muševič. Colloidal entanglement in highly twisted chiral nematic colloids: Twisted loops, Hopf links, and trefoil knots. *Phys. Rev. E*, 84:031703, 2011.
 - [106] Y. Bouligand. Recherches sur les textures des états mésomorphes: Dislocations coins et signification des cloisons de Grandjean-Cano dans les cholestériques. *J. Phys. France*, 35:959, 1974.
 - [107] Jung-Shen B. Tai and Ivan I. Smalyukh. Three-dimensional crystals of adaptive knots. *Science*, 365:1449, 2019.
 - [108] M. Škarabot, M. Ravnik, S. Žumer, U. Tkalec, I. Poberaj, D. Babič, N. Osterman, and I. Muševič. Two-dimensional dipolar nematic colloidal crystals. *Phys. Rev. E*, 76:51406, 2007.

- [109] M Škarabot, M Ravnik, S Žumer, U Tkalec, I Poberaj, D Babič, N Osterman, and I Mušević. Interactions of quadrupolar nematic colloids. *Phys. Rev. E*, 77(3):31705, 2008.
- [110] Muhammed M Rasi, Ravi Kumar Pujala, and Surajit Dhara. Colloidal analogues of polymer chains, ribbons and 2d crystals employing orientations and interactions of nano-rods dispersed in a nematic liquid crystal. *Sci. Rep.*, 9:401001, 2019.
- [111] Clayton P. Lapointe, Sharla Hopkins, Thomas G. Mason, and Ivan I. Smalyukh. Electrically Driven Multiaxis Rotational Dynamics of Colloidal Platelets in Nematic Liquid Crystals. *Phys. Rev. Lett.*, 105:178301, 2010.
- [112] Angel Martinez, Leonardo Hermosillo, Mykola Tasinkevych, and Ivan I. Smalyukh. Linked topological colloids in a nematic host. *Proc. Natl. Acad. Sci.*, 112:4546, 2015.
- [113] Clayton P. Lapointe, Kenny Mayoral, and Thomas G. Mason. Star colloids in nematic liquid crystals. *Soft Matter*, 9:7843, 2013.
- [114] Bohdan Senyuk, Qingkun Liu, Ephraim Bililign, Philip D. Nystrom, and Ivan I. Smalyukh. Geometry-guided colloidal interactions and self-tiling of elastic dipoles formed by truncated pyramid particles in liquid crystals. *Phys. Rev. E*, 91:040501, 2015.
- [115] Bohdan Senyuk, Manoj B. Pandey, Qingkun Liu, Mykola Tasinkevych, and Ivan I. Smalyukh. Colloidal spirals in nematic liquid crystals. *Soft Matter*, 11:8758, 2015.
- [116] Dinesh Kumar Sahu, Thriveni G. Anjali, Madivala G. Basavaraj, Jure Aplinc, Simon Čopar, and Surajit Dhara. Orientation, elastic interaction and magnetic response of asymmetric colloids in a nematic liquid crystal. *Sci. Rep.*, 9:1557, 2019.
- [117] Ye Yuan, Angel Martinez, Bohdan Senyuk, Mykola Tasinkevych, and Ivan I. Smalyukh. Chiral liquid crystal colloids. *Nat. Mater.*, 17:71, 2017.
- [118] S. M. Hashemi, U. Jagodič, M. R. Mozaffari, M. R. Ejtehad, I. Mušević, and M. Ravnik. Fractal nematic colloids. *Nat. Commun.*, 8:14026, 2017.
- [119] Qian Zhao, Lei Kang, Bo Du, Bo Li, Ji Zhou, Hong Tang, Xiao Liang, and Baizhe Zhang. Electrically tunable negative permeability metamaterials based on nematic liquid crystals. *Appl. Phys. Lett.*, 90:011112, 2007.
- [120] Jure Aplinc, Anja Pusovnik, and Miha Ravnik. Designed self-assembly of metamaterial split-ring colloidal particles in nematic liquid crystals. *Soft Matter*, 15:5585, 2019.
- [121] Mingkai Liu, Kebin Fan, Willie Padilla, David A. Powell, Xin Zhang, and Ilya V. Shadrivov. Tunable Meta-Liquid Crystals. *Adv. Mater.*, 28:1553, 2016.
- [122] Xian Chen, Irene Fonseca, Miha Ravnik, Valeriy Slastikov, Claudio Zannoni, and Arghir Zarnescu. Topics in the mathematical design of materials. *Phil. Trans. R. Soc. A*, 379:20200108, 2021.
- [123] Mohamed Amine Gharbi, Marcello Cavallaro, Gaoxiang Wu, Daniel A. Beller, Randall D. Kamien, Shu Yang, and Kathleen J. Stebe. Microbullet assembly: interactions of oriented dipoles in confined nematic liquid crystal. *Liq. Cryst.*, 40:1619, 2013.
- [124] Kazumasa A Takeuchi and Masaki Sano. Universal {Fluctuations} of {Growing} {Interfaces} {Evidence} in {Turbulent} {Liquid} {Crystals}. *Phys. Rev. Lett.*, 104:230601, 2010.
- [125] Oliver Wiese, Davide Marenduzzo, and Oliver Henrich. Microfluidic flow of cholesteric liquid crystals. *Soft Matter*, 12:9223, 2016.
- [126] Z Dogic and S Fraden. Ordered phases of filamentous viruses. *Curr. Opin. Colloid Interface Sci.*, 11:47, 2006.
- [127] Jure Aplinc, Mitja Štimulak, Simon Čopar, and Miha Ravnik. Nematic liquid crystal gyroids as photonic crystals. *Liq. Cryst.*, 43:2320, 2016.
- [128] Ž. Kos, M. Ravnik, and S. Žumer. Nematodynamics and structures in junctions of cylindrical micropores. *Liq. Cryst.*, 44:2161–2171, 2017.
- [129] Luca Giomi, Ž Kos, Miha Ravnik, and Anupam Sengupta. Cross-talk between topological defects in different fields revealed by nematic microfluidics. *Proc. Natl. Acad. Sci.*, 114:E5771, 2017.
- [130] Takeaki Araki. Dynamic coupling between a multistable defect pattern and flow in nematic liquid crystals confined in a porous medium. *Phys. Rev. Lett.*, 109:257801, 2012.
- [131] Anupam Sengupta, Christoph Pieper, Jörg Enderlein, Christian Bahr, and Stephan Herminghaus. Flow of a nematogen past a cylindrical micro-pillar. *Soft Matter*, 9:1937, 2013.
- [132] Yimin Luo, Daniel A. Beller, Giuseppe Boniello, Francesca Serra, and Kathleen J. Stebe. Tunable colloid trajectories in nematic liquid crystals near wavy walls. *Nat. Commun.*, 9:1253751, 2018.
- [133] Simon Čopar, Žiga Kos, Tadej Emeršič, and Uroš Tkalec. Microfluidic control over topological states in channel-confined nematic flows. *Nat. Commun.*, 11:977, 2020.
- [134] Darja Lisjak and Alenka Mertelj. Anisotropic magnetic nanoparticles: A review of their properties, syntheses and potential applications. *Progress in Materials Science*, 95:286, 2018.